Available online at www.sciencedirect.com

ScienceDirect

journal homepage: www.elsevier.com/locate/he

# Promoted hydrogen generation from formic acid with amines using $Au/ZrO_2$ catalyst

Qing-Yuan Bi [a,b], Jian-Dong Lin [a], Yong-Mei Liu [a], Fu-Qiang Huang [b,c], Yong Cao [a,*]

[a] Department of Chemistry, Shanghai Key Laboratory of Molecular Catalysis and Innovative Materials, Collaborative Innovation Center of Chemistry for Energy Materials, Fudan University, Shanghai 200433, PR China
[b] State Key Laboratory of High Performance Ceramics and Superfine Microstructure, Shanghai Institute of Ceramics, Chinese Academy of Sciences, Shanghai 200050, PR China
[c] Beijing National Laboratory for Molecular Sciences and State Key Laboratory of Rare Earth Materials Chemistry and Applications, College of Chemistry and Molecular Engineering, Peking University, Beijing 100871, PR China

ARTICLE INFO

*Article history:*
Received 31 May 2016
Received in revised form
20 September 2016
Accepted 21 September 2016
Available online 8 October 2016

*Keywords:*
Formic acid
Hydrogen
Organic amine
$Au/ZrO_2$ catalyst
Promoting effect

ABSTRACT

Decomposition of formic acid (FA) to hydrogen and carbon dioxide through catalysis holds great promise for clean energy in fuel cells designed for portable use, but the selective and efficient dehydrogenation of FA by a robust heterogeneous catalyst under ambient conditions remains a major challenge. We report herein that a new FA dehydrogenation system comprising liquid FA and amines with high boiling point as hydrogen storage material can be efficiently decomposed for ultrapure $H_2$ release under mild reaction conditions. Of significant importance is that a high turnover frequency (TOF) of up to 1166 $h^{-1}$ can be readily attained at 60 °C in FA-dimethylethanolamine system using gold nanoparticles supported on amphoteric zirconia ($Au/ZrO_2$). The amine acts as a proton scavenger can facilitate the O–H bond cleavage in the key step of FA deprotonation in Au–$ZrO_2$ interface resulting in high catalytic activity. The versatile gold catalyst displayed excellent stability for dimethylethanolamine-assisted FA dehydrogenation as well as a typical particle-size-dependent effect.



## Introduction

Hydrogen, a green energy vector, has been considered as an ideal potential candidate to solve both the global energy and environmental problems [1–4]. However, because of its low boiling point and low volumetric energy density at atmospheric conditions, $H_2$ is difficult to store in compressed or liquid form and hard to transport with safe manner, and these are both of the major challenges in establishing a hydrogen economy [5,6]. Although many porous materials can be used for physical hydrogen storage, hydrogen capacities of the materials limit their further applications [7–10]. In chemical hydrogen storage, formic acid (HCOOH, FA) has been identified as one of the most important liquid compounds for safe and convenient hydrogen storage in fuel cells designed for portable use owing to its considerable

* *Corresponding author*. Fax: +86 21 65643774.
E-mail address: yongcao@fudan.edu.cn (Y. Cao).
http://dx.doi.org/10.1016/j.ijhydene.2016.09.150

hydrogen content (53 g $L^{-1}$), nontoxicity and high stability under ordinary conditions [11–15]. It is known that the chemical decomposition of FA proceeds via two main pathways, i.e., the dehydrogenation process to form $H_2$ and $CO_2$, and the dehydration one to form $H_2O$ and CO (Scheme 1) [16–20]. Under the design and preparation of catalyst used, the activity and selectivity of hydrogen generation can be strongly controlled and the production of CO impurity can also be strictly constrained.

Much progress has been made both on the homogeneous and heterogeneous catalysis for the selective dehydrogenation of FA [21–49]. And the heterogeneous catalysts have attracted increasing interest owing to the advantage of operating at ambient atmosphere as well as facile separation and recycling [28–49]. In an overview of literature, Au and Pd are more active than other analogous solids [28–49]. Xu et al. grafted the electron-rich functional group ethylenediamine (ED) into metal-organic frameworks (MOFs) MIL-101 to immobilize bimetallic Au–Pd nanoparticles (NPs) showing the turnover frequency (TOF) of 106 $h^{-1}$ at 90 °C [31]. A trimetallic PdAuEu/C was demonstrated by Xing and co-workers displayed the activity of 387 $h^{-1}$ at 92 °C for FA dehydrogenation [28]. However, the high performance observed from these catalysts could only be achieved at high temperatures (>80 °C) for liquid FA decomposition and the kinetic properties of FA dehydrogenation under ambient conditions still need to be further promoted. Apart from the optimization of catalysts, great efforts have also been made on the development of FA decomposing reaction system [28,31–34,50]. For example, extra additives, such as various organic amines and sodium formate or potassium formate were conventionally used as proton scavenger to facilitate the O–H bond cleavage and thus leading to the formation of a metal-formate species during the initial step of the overall dehydrogenation process [28,31–34,50].

More recently, we have found that a simple Au-based catalyst (Au/$ZrO_2$) can efficiently release the $H_2$ stored in liquid FA under ambient conditions [50]. With this versatile gold material, controlled and efficient CO-free $H_2$ liberation from a FA-amine (FA/$NEt_3$ with molar ratio of 5/2) mixture can be readily achieved. However, the promoter of $NEt_3$ with low boiling point (89.5 °C) can be volatilized in the FA decomposition process and the generated $H_2$ gas with volatile organic compounds (VOCs) could not be directly adapted to downstream practical applications such as fuel-cell-based technologies for clean power generation [50]. Therefore, it is necessary to search a base promoter with high boiling point to assist FA dehydrogenation showing no or extremely trace volatile gas. Herein, we present a profile for screening assisted amines with high boiling point for promoting hydrogen generation from FA and describe the influence of organic bases on the activity of the Au-catalyzed dehydrogenation of FA. Besides the nature of the amine, its ratio to FA also controls the performance of the catalyst system.

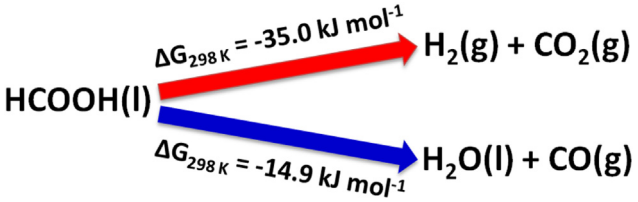


**Scheme 1 – Two pathways of formic acid decomposition.**

## Experimental

### *Catalyst preparation*

$ZrO_2$ (56% monoclinic and 44% tetragonal phase) powders were prepared with a conventional precipitation method following the previous procedure [50]. 8.0 g zirconium oxychloride octahydrate ($ZrOCl_2 \cdot 8H_2O$, Alfa Aesar, 99%) was dissolved in 200 mL deionized water and the pH was adjusted to approximately 9.5 by dropwise addition of 2.5 M $NH_3 \cdot H_2O$ (Aldrich, 28%) under stirring at room temperature. The resultant hydrogel was thoroughly washed with deionized water until free of $Cl^-$ after stirring for 8 h. The precipitate was then dried at 100 °C for 12 h followed by calcination at 400 °C (ramping rate of 10 °C $min^{-1}$) in air for 2 h to obtain the final material.

A modified deposition-precipitation (DP) procedure has been used to prepare the Au/$ZrO_2$ samples [50]. Briefly, 2.0 g $ZrO_2$ powders were dissolved with 100 mL 1 mM (or 1.6 mM) of aqueous solution of $HAuCl_4$ (Alfa Aesar, 48 wt% Au), and the pH was adjusted to 9.0 by dropwise addition of 0.25 M $NH_3 \cdot H_2O$ (CAUTION: the addition of $NH_3 \cdot H_2O$ to $HAuCl_4$ solution may give rise to highly explosive fulminating gold). After 6 h (or 12 h or 24 h) stirring at room temperature, the catalyst was washed six times with deionized water until free of $Cl^-$ (using $AgNO_3$ solution for test) and separated by filtration. The samples were dried at 110 °C in air for 1 h, followed by a careful treatment with a stream of 5 vol% $H_2$/Ar at 300 °C (ramping rate of 5 °C $min^{-1}$) for 2 h. The Au loading was determined to be 0.8 wt% by ICP-AES.

The Au/$ZrO_2$ catalyst with subnanometric gold particle size of about 0.8 nm was prepared following the abovementioned method under milder conditions [50]. Basically, 1.0 g $ZrO_2$ powder was dispersed into 200 mL 0.25 mM of aqueous solution of $HAuCl_4$, the pH of which was adjusted to 9.0 by dropwise addition of 0.25 M $NH_3 \cdot H_2O$. After 6 h stirring at room temperature, the catalyst was washed six times with deionized water until free of $Cl^-$ (using $AgNO_3$ solution for test) and separated by filtration. The sample was then dried at 25 °C under vacuum for 12 h, followed by a careful treatment with a stream of 5 vol% $H_2$/Ar at 250 °C (ramping rate of 5 °C $min^{-1}$) for 2 h.

### *Catalyst characterization*

The BET specific surface areas of the catalysts were determined by adsorption–desorption of nitrogen at −196 °C, using a Micromeritics TriStar 3000 equipment. Sample degassing was performed at 300 °C prior to acquiring the adsorption isotherm. Actual Au loading of the catalysts was measured by using inductively coupled plasma atomic emission spectroscopy (ICP-AES) with a Thermo Electron

IRIS Intrepid II XSP spectrometer. XRD operation of the catalysts was carried out on the German Bruker D8 Advance X-ray diffractometer with Ni filtered Cu Kα radiation at 40 kV and 20 mA. XPS data were collected with a Perkin Elmer PHI 5000C system equipped with a hemispherical electron energy analyzer. The spectrometer was performed at 15 kV and 20 mA, and the Mg anode (Mg Kα, hν = 1253.6 eV) was used. The C 1s line (284.6 eV) was used as reference to calculate the binding energies (BE). A JEOL 2011 microscope operating at 200 kV with an EDX unit (Si(Li) detector) was used for TEM investigations. The samples were prepared by grinding and subsequent dispersing the powder into ethanol and applying a drop of very dilute suspension on the carbon-coated grids.

CO concentration with very low levels in FA-amine adducts dehydrogenation can be reliably measured by using a GC (Agilent 6890) analysis system equipped with a methanizer and a FID (detection limit ~ 1.0 ppmv). More operation details can be found elsewhere [50].

CO chemisorption measurements were performed at −116 °C [51]. A homemade equipment was used for pulse chemisorption. In principle the system was made of a U-shaped quartz reactor equipped with an oven controlled by a PID temperature programmer, mass flow meters, sampling valve, a quadrupole mass detector. Before chemisorption the following standard pretreatment procedure was applied: the sample (200 mg) was reduced in $H_2$ flow (40 mL $min^{-1}$) at 250 °C for 30 min, cooled in $H_2$ to ambient temperature, purged in He flow and finally hydrated at ambient temperature. The hydration treatment was performed by contacting the sample with a He flow (10 mL $min^{-1}$) saturated with water. The sample was then cooled in He flow to −116 °C (attained and maintained by an ethanol-liquid nitrogen cryogenic mixture in a Dewar flask) for CO chemisorption. For standard measurements the following operating conditions are recommended: CO content in pulses (5 vol%), helium flow rate (30 mL $min^{-1}$), pulse size (0.5 mL), time interval between pulses (4 min).

### *Catalytic activity test*

All catalytic experiments were carried out in open system under ambient atmosphere of air. The reactions were performed in a double-walled thermostatically controlled reaction vessel of 10 mL under steady magnetic stirring of 800 rpm at given temperatures (40–80 °C) with a reflux condenser, which is connected to an automatic gas burette, where the gases can be collected. The gas burette is equipped with a pressure sensor. Gas evolved during the reaction causes a pressure increase in the reaction system, which is compensated by the volume increase of the burette syringe with an automatic controlling unit. The gas evolution curves can be collected by a personal computer. There is a two piston burette for the measurements above 100 mL. For the large-scale hydrogen generation from FA-amine adducts, the reaction was performed in the vessel of 50 mL. In addition, the generated gas was qualitatively and quantitatively analyzed by the GC (Agilent 6820 with a TDX-01 column connected to a TCD). Typically, a ratio of $H_2$ to $CO_2$ of 1:1 (±5%) is detected. The initial turnover frequency (first 20 min) based on total gold atoms (TOF) and surface gold atoms ($TOF_{surface}$) were respectively calculated as follows:

$$TOF = \frac{\text{generated } H_2\,(\text{mol})}{\text{total Au atoms}\,(\text{mol}) \times \text{time}\,(\text{h})}$$

$$TOF_{surface} = \frac{\text{generated } H_2\,(\text{mol})}{\text{surface Au atoms}\ \,(\text{mol}) \times \text{time}\,(\text{h})}$$

For the reuse experiment, the centrifuged catalysts from the parallel activity tests were collected and washed thoroughly with deionized water, followed by drying at 110 °C in air for 1 h and reduction treatment by a stream of 5 vol% $H_2$/Ar at 300 °C (ramping rate of 5 °C $min^{-1}$) for 2 h. All catalytic activity tests were carried out following the same procedure as abovementioned. To verify whether there is any leaching of Au or $ZrO_2$ during the catalytic decomposition, the Au/$ZrO_2$ catalyst was removed from the reaction mixture by using filtration after 3 h reaction. Analysis of the filtrate with ICP-AES showed no detectable leaching of Zr or Au (<2.5 ppb) into the solution.

## Results and discussion

### *Promoted hydrogen generation from formic acid with amines using Au/$ZrO_2$ catalyst*

We firstly prepared the Au/$ZrO_2$ catalyst with gold particle size of *ca.* 1.8 nm with modified DP method, the physical and textural properties of Au/$ZrO_2$ have been described in our previous work [50]. Au/$ZrO_2$ displayed excellent performance for hydrogen generation from FA-$NEt_3$ adducts, but the inevitable factor of low boiling point of $NEt_3$ limits its practical application in fuel-cell-based technologies. In the course of our continuing efforts in searching promoter amine with high boiling point for efficient FA dehydrogenation, we screened many kinds of amine for the goal transformation under mild conditions. In control experiment at 60 °C, only little hydrogen generation is observed over Au/$ZrO_2$ in the absence of amine (Table 1, entry 1). Other amines, such as diethanolamine, triethanolamine, dimethylethanolamine, tetramethylethylenediamine and dimethyl-*n*-butylamine can greatly promote the dehydrogenation efficiency (Table 1, entries 2–6). The amine acts as a proton scavenger can facilitate the O–H bond cleavage in the key step of FA deprotonation in Au–$ZrO_2$ interface resulting in high catalytic activity [50]. It can be seen that tertiary amines showed more significant promoting effect for FA dehydrogenation. After a preliminary screening, dimethylethanolamine with much higher boiling point than $NEt_3$ displayed the most promoting effect for FA-amine adducts decomposition with generated gas of more than 394 mL in 3 h and the initial TOF of 1166 $h^{-1}$ (Table 1, entry 4). Meanwhile, the CO concentration was less than 10 ppm and no detection of VOCs in the evolved gaseous mixture for Au/$ZrO_2$ catalyzed dehydrogenation at 60 °C, which are crucial for generated $H_2$ in the downstream fuel-cell-based technologies. It should be noted that the promoted effect of dimethylethanolamine on

**Table 1 – Study of various organic amines for the generation of $H_2$ via FA-amine system decomposition by using $Au/ZrO_2$ catalyst.[a]**

$$HCOOH \xrightarrow[Amine]{Cat., T} H_2 + CO_2$$

| Entry | Amine | Boiling point (°C)[b] | $V_{gas}$ (mL) | TOF ($h^{-1}$)[c] | TON[d] |
|---|---|---|---|---|---|
| 1[e] | Water | 100 | 34.6 | 211 | 123 (187) |
| 2 | Diethanolamine | 269 | 202.3 | 605 | 477 (1094) |
| 3 | Triethanolamine | 360 | 272.2 | 812 | 626 (1472) |
| 4 | Dimethylethanolamine | 135 | 394.5 | 1166 | 926 (2133) |
| 5 | Tetramethylethylenediamine | 122 | 339.4 | 950 | 841 (1835) |
| 6 | Dimethyl-*n*-butylamine | 95 | 222.5 | 698 | 559 (1203) |

[a] Reaction conditions: 5.0 mL scale of FA/amine system (53.0 mmol FA, 21.2 mmol amine), 3.75 μmol Au, 60 °C, 3 h.
[b] The boiling point of amine.
[c] Initial TOF after 20 min.
[d] TON for 1 h, numbers in parentheses refer to TON for 3 h.
[e] 5.0 mL scale of 10.5 M aqueous FA.

FA dehydrogenation was similar with $NEt_3$ and the performance of $Au/ZrO_2$ for FA-dimethylethanolamine adducts was about 5.5 times higher than that of the amine-free counterpart and comparable with the most active heterogeneous catalyst systems previously reported under mild conditions [28,31–34,40–43,48–50]. Furthermore, the durability of gold catalyst in FA-amine adducts is better than in aqueous FA system according to the turnover number (TON) parameters. These results suggested that the secondary and tertiary amines can promote hydrogen generation from FA using supported gold catalyst and dimethylethanolamine was the most effective promoter.

To measure the ease of the amine-promoted liquid FA dehydrogenation catalyzed by the $Au/ZrO_2$ catalyst, we recorded the conversion profile and reaction rate of $H_2$ generation at different temperatures (40–80 °C) in the presence of 53.0 mmol FA and 21.2 mmol amine, as shown in Fig. 1. Low temperature was hard to stimulate the catalytic potential of $Au/ZrO_2$ for any amine assisted FA dehydrogenation, and elevated temperatures can steadily improve the efficiency. At one given temperature, the promoting effect of dimethylethanolamine for FA dehydrogenation was largest with the FA conversion of more than 50% at 80 °C in 3 h. By plotting the logarithmic TOF vs. 1/T, we obtained the Arrhenius plot (Fig. 2). From the linear Arrhenius behavior, we calculated the apparent activation energy ($E_a$) to be 20.8, 24.3, 27.4, 34.9 and 35.6 kJ $mol^{-1}$ for dimethylethanolamine, tetramethylethylenediamine, triethanolamine, dimethyl-*n*-butylamine and diethanolamine promoted FA dehydrogenation over $Au/ZrO_2$ catalyst, respectively. These are lower than most of reported data for FA dehydrogenation catalyzed by heterogeneous catalysts [28–50]. The different $E_a$ indicates that the amines

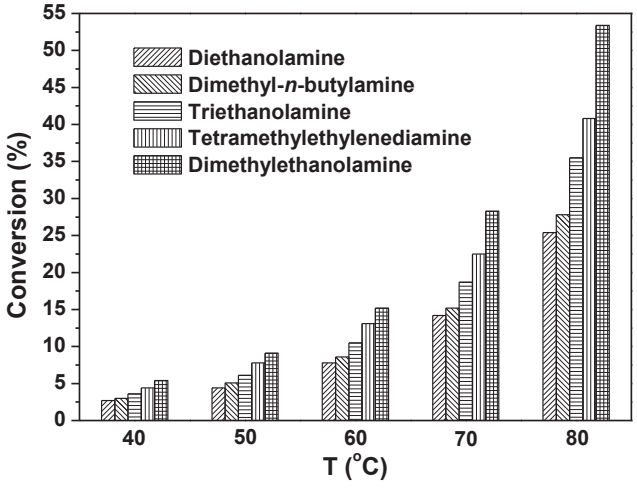


**Fig. 1 – Conversion of formic acid as a function of temperature using $Au/ZrO_2$ catalyst. Reaction conditions: 5.0 mL scale of FA/amine system (53.0 mmol FA, 21.2 mmol amine), 3.75 μmol Au, 3 h.**

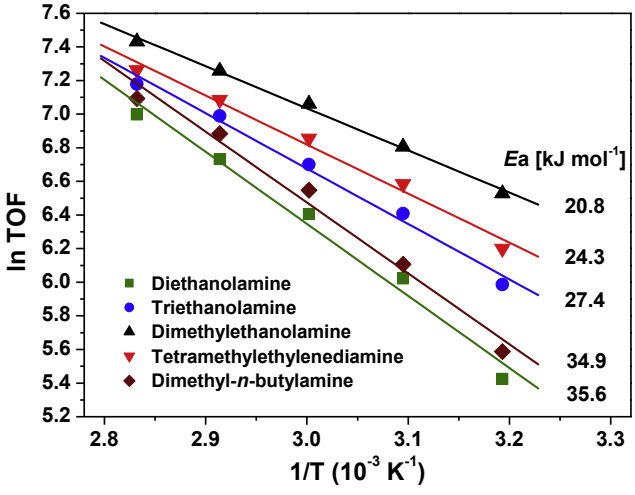


**Fig. 2 – Arrhenius plots for $Au/ZrO_2$ catalyzed hydrogen evolution from the FA/amine systems. Reaction conditions: 5.0 mL scale of FA/amine system (53.0 mmol FA, 21.2 mmol amine), 3.75 μmol Au, 20 min.**

with various structures showed different impact on FA decomposition and dimethylethanolamine with unique tertiary form could readily interact with FA molecules in the key step of FA deprotonation in Au–$ZrO_2$ interface and easily overcome the low activation barrier for achieving high dehydrogenation performance.

The concentration of the amine also strongly affects the rate of hydrogen generation. We investigated the effect of these amines and the concentrations in more detail. There was low catalytic activity for hydrogen evolution in the absence of amine and an increasing concentration was beneficial for hydrogen production. It turned out to be a volcano-shaped relationship between reaction rate and FA/amine molar ratio, as shown in Fig. 3. For alcamines, including dimethylethanolamine, triethanolamine and diethanolamine, the rates of $H_2$ generation increased as amine concentration increasing from FA/amine molar ratio of 9/1 to 2.5/1; however, more amines (FA/amine molar ratio > 2.5) were found to give a negative effect on dehydrogenation kinetics. For tetramethylethylenediamine and dimethyl-*n*-butylamine, the peak value of the amine promoted effect was appeared at 1.5/1 and 1/1, respectively. These results reveal that suitable amount of amine plays an indispensable role in the catalytic dehydrogenation of FA over Au/$ZrO_2$ catalyst.

Having established that FA-dimethylethanolamine with the FA/amine molar ratio of 2.5 as a reliable and efficient system for chemical hydrogen storage, we further investigated the reusability of Au catalyst under mild conditions. As shown in Fig. 4, Au/$ZrO_2$ was recoverable by simple filtration and proven robust even after five reuses. Noteworthy, the gas production rate of the 2nd run was only marginally lower than the fresh catalyst in the 1st run and kept a constant value in the later reuses. Furthermore, the phase transformation of $ZrO_2$ support, change of Au surface metallic nature and remarkable sintering of Au NPs during real reaction process were not observed (Fig. 5). Au/$ZrO_2$ was removed from the reaction mixture at 15% of FA conversion. Further processing

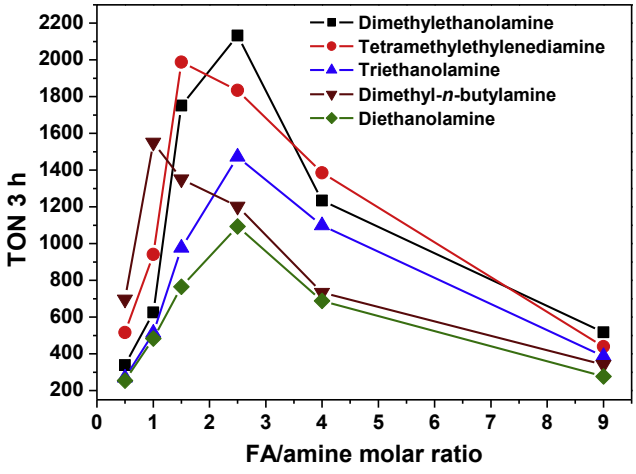


**Fig. 3 – TON as a function of the FA/amine molar ratio using Au/$ZrO_2$ catalyst. Reaction conditions: 5.0 mL scale of FA/amine system, n(FA)/n(Au) = 14000, 60 °C, 3 h.**

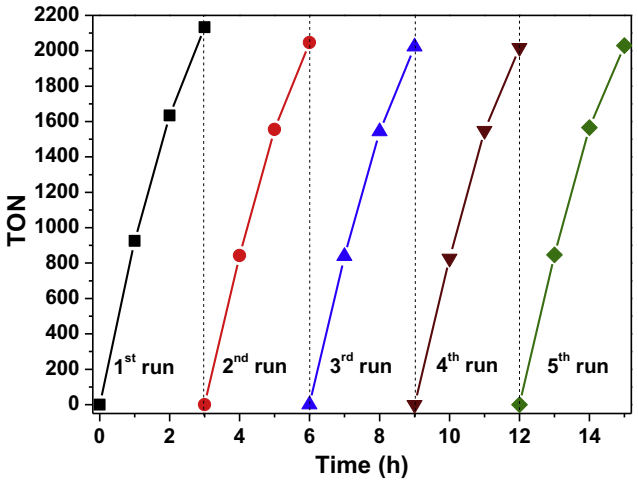


**Fig. 4 – Reuse of the Au/$ZrO_2$ catalyst for hydrogen generation via decomposition of FA/dimethylethanolamine system. Reaction conditions: 5.0 mL scale of 53.0 mmol FA and 21.2 mmol dimethylethanolamine, 3.75 μmol Au, 60 °C, 3 h in each run.**

of the filtrate at 60 °C for 1 h did not result in any gas release. In addition, ICP-AES analysis of the filtrate confirmed that the content of Au in the solution was below the detection limit. To our delight, the Au/$ZrO_2$ still displayed excellent large-scale stability for $H_2$ generation in 20.0 mL of 5FA-2dimethylethanolamine system, as shown in Fig. 6. Emphasized that the decline of reaction rate in longer time was mainly due to the consumption of FA and the destruction of initial molar balance. These results indicate that Au/$ZrO_2$ was very robust for dimethylethanolamine-promoted FA dehydrogenation and could keep its intrinsic nature of heterogeneous catalysis in overall reaction.

### *Effect of Au particle size on formic acid dehydrogenation*

It is well known that the size of Au NPs significantly affects their catalytic behavior in many reactions [50–55]. It was found that the mean size of Au NPs in Au/$ZrO_2$ catalyst could be easily regulated in the range of subnano scale to approximately 10 nm by changing the concentration of the gold precursor ($HAuCl_4$) and/or the ageing time during the preparation process with DP method [52]. Fig. 7 shows the TEM images of various Au/$ZrO_2$ catalysts with different mean sizes of Au NPs on the varied preparation conditions. It is difficult to obtain the image of the gold subnanoclusters supported on $ZrO_2$ owing to the poor contrast, but the cluster size can be determined by the method of low temperature CO chemisorption was *ca.* 0.8 nm [50,51]. The typical TEM micrographs and particle-size distributions of Au/$ZrO_2$ catalysts with mean-size of 3.5, 6.8, and 9.6 nm are shown in Fig. 7.

The initial $HAuCl_4$ solution with higher concentration and the expanded ageing time but with a fixed Au amount in the solution can increase the adsorption of Au-

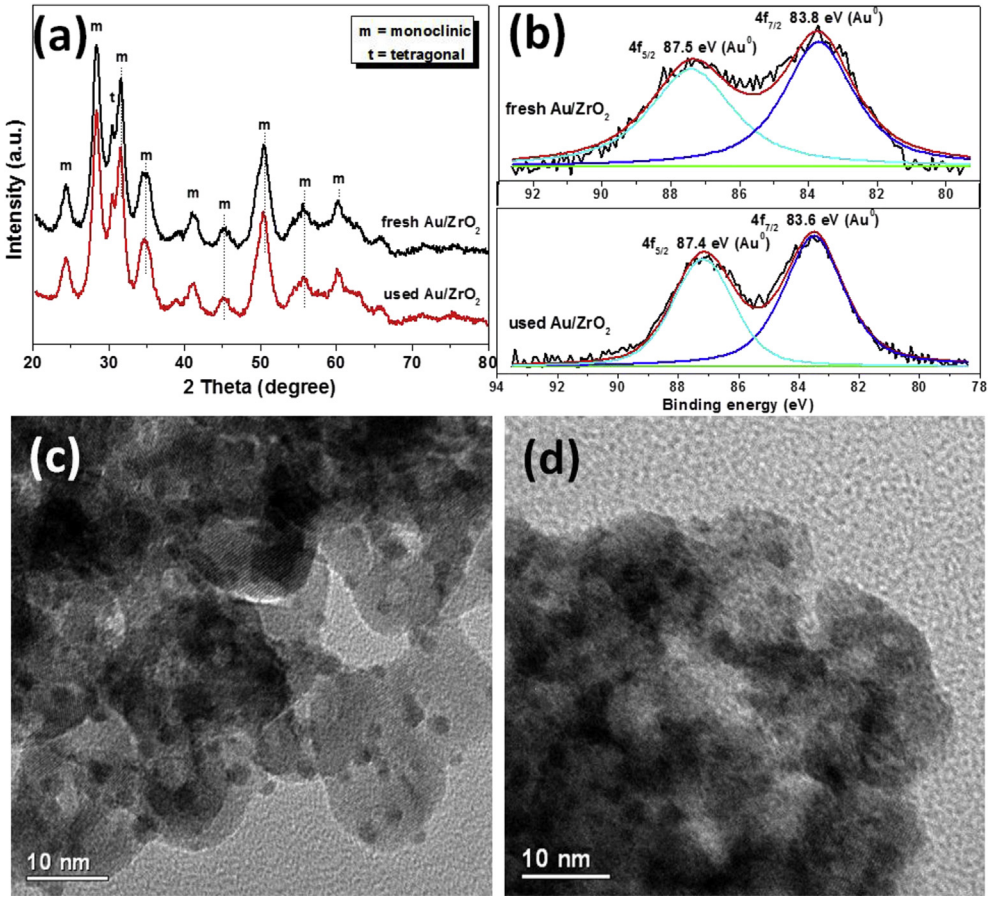


**Fig. 5 – (a) XRD patterns, (b) XPS data of $Au^0$, and TEM images of (c) fresh and (d) used $Au/ZrO_2$ catalyst after five runs.**

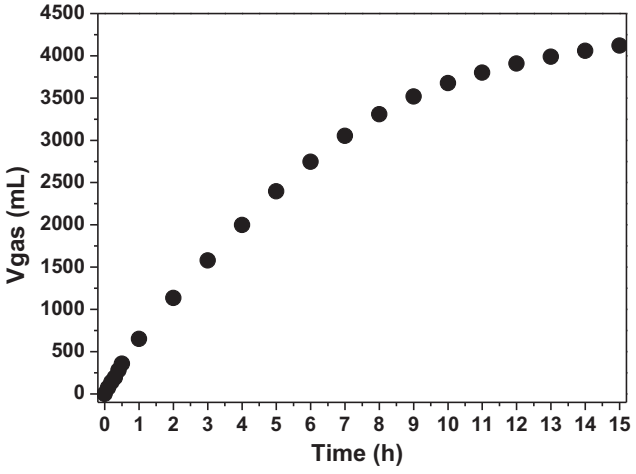


**Fig. 6 – Large-scale hydrogen generation from FA/dimethylethanolamine system using $Au/ZrO_2$ catalyst. Reaction conditions: 20.0 mL scale of 212.0 mmol FA and 84.8 mmol dimethylethanolamine, 15.0 μmol Au, 60 °C.**

containing precursor on the underlying support during the stirring and subsequently increase the surface density of Au atoms after thermal reduction process [52]. The larger Au NPs can be formed with instantaneous nucleation and continuous growth and the post-treatment due to the accumulation of Au atoms. Table 2 lists the effect of preparation conditions on the size of Au NPs and further on the activity for FA-dimethylethanolamine adducts dehydrogenation. It can be seen that the higher concentration of initial $HAuCl_4$ solution and/or the longer ageing time, the larger size of the Au NPs. With the increase of Au NPs, the $Au/ZrO_2$ catalyst exhibited decreased performance for FA dehydrogenation markedly from evolved gas in 3 h of 632.3 mL for 0.8 nm to of 115.8 mL for 6.8 ± 0.3 nm, as listed in Table 2. The catalytic ability of 9.6 ± 0.4 nm Au NPs supported on $ZrO_2$ was the lowest, showing the TOF of only 105 $h^{-1}$ at 60 °C. Interestingly, there is an intrinsic consistency of the relationship on size effect of Au NPs between dehydrogenation performance and the surface gold active sites ($TOF_{surface}$), as shown in Fig. 8b, indicative of the origin of gold catalysis in small molecule activation and transformation. These results demonstrate that the FA-dimethylethanolamine dehydrogenation over $Au/ZrO_2$ is a typical particle-size-dependent reaction.

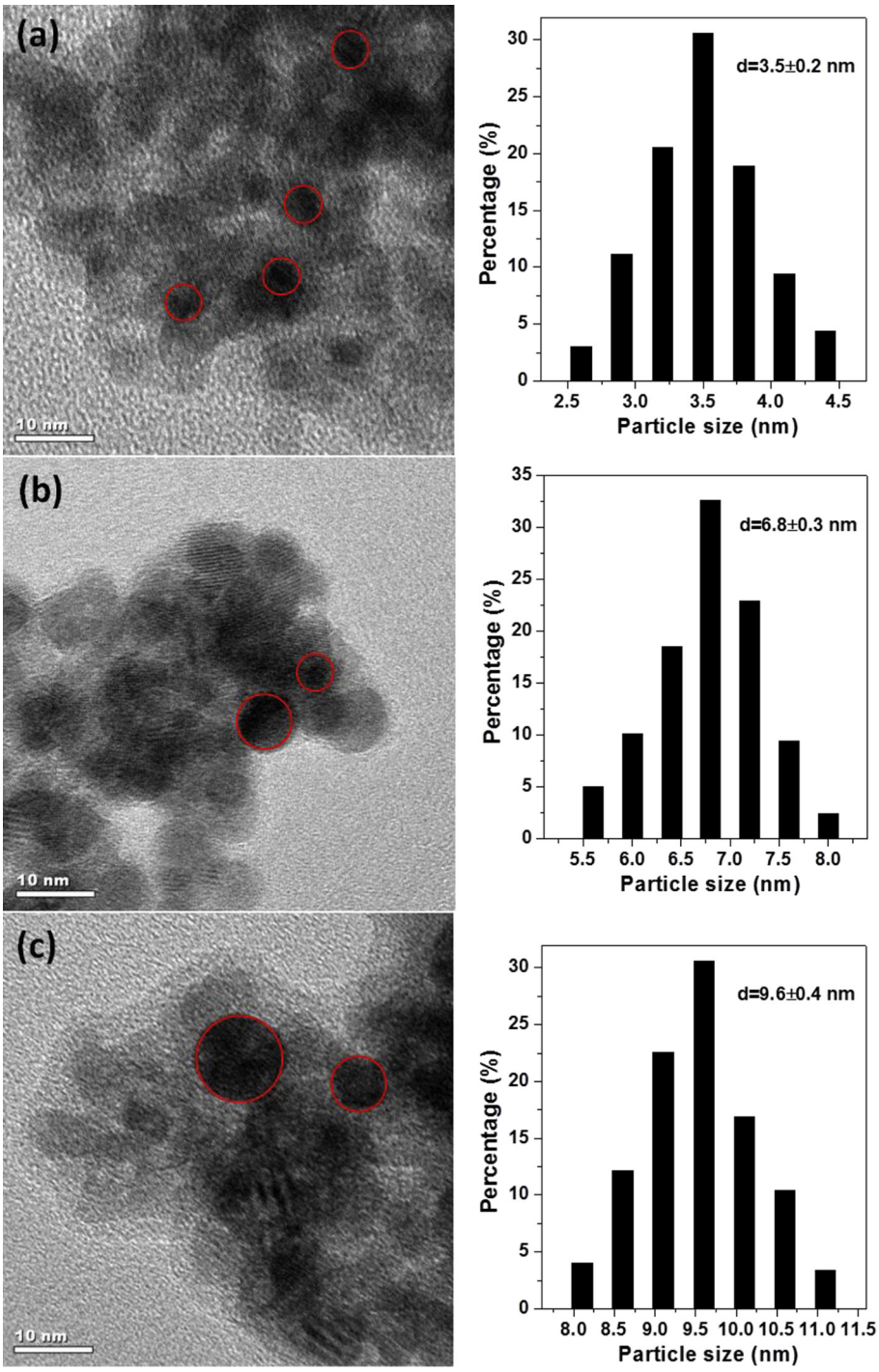


**Fig. 7 – Typical TEM micrographs and particle-size distributions for the $Au/ZrO_2$ catalysts with mean-size of (a) 3.5, (b) 6.8, and (c) 9.6 nm.**

**Table 2 – Effect of preparation conditions on $Au/ZrO_2$ catalyst for FA dehydrogenation.[a]**

| Entry | $[HAuCl_4]$ (mM) | Ageing time (h) | Mean size of Au NPs (nm)[b] | Dispersion (%)[c] | TOF ($h^{-1}$)[d] | $V_{gas}$ (mL) |
|---|---|---|---|---|---|---|
| 1 | 0.25 | 6 | 0.8[e] | 95.1 | 2015 | 632.3 |
| 2 | 1.0 | 6 | 1.8 ± 0.1 | 60.8 | 1166 | 394.5 |
| 3 | 1.6 | 6 | 3.5 ± 0.2 | 39.4 | 857 | 291.6 |
| 4 | 1.6 | 12 | 6.8 ± 0.3 | 16.2 | 328 | 115.8 |
| 5 | 1.6 | 24 | 9.6 ± 0.4 | 5.3 | 105 | 36.6 |

[a] The Au loading was fixed at 0.8 wt%. Reaction conditions: 5.0 mL scale of 53.0 mmol FA and 21.2 mmol dimethylethanolamine, 3.75 μmol Au, 60 °C, 3 h.
[b] Determined from TEM.
[c] Dispersion calculated according to the data of CO chemisorption at −116 °C. Assuming an equal Au/CO chemisorption stoichiometry for gold NPs or subnano-clusters dispersed on $ZrO_2$ support, the size was calculated based on an assumption of a quasi-hemispherical model of gold particle as referred in Ref. [50].
[d] Initial TOF after 20 min.
[e] Measured by CO chemisorption at −116 °C.

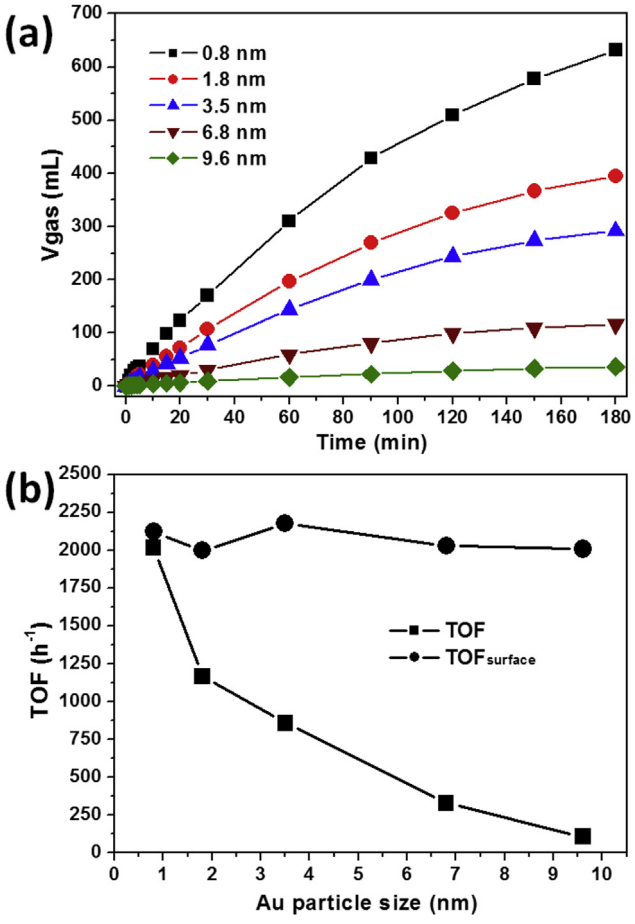


**Fig. 8 – (a) Hydrogen evolution and (b) TOF and $TOF_{surface}$ of $Au/ZrO_2$ with different Au particle size for dehydrogenation of FA/dimethylethanolamine. Reaction conditions: 5.0 mL scale of 53.0 mmol FA and 21.2 mmol dimethylethanolamine, 3.75 μmol Au, 60 °C, 3 h.**

## Conclusions

We have developed a new FA dehydrogenation system comprising liquid FA and amine with high boiling point as hydrogen storage material which can be efficiently decomposed for ultrapure $H_2$ gas under mild reaction conditions using gold nanoparticles supported on amphoteric zirconia catalyst ($Au/ZrO_2$). The amine acts as a proton scavenger can facilitate the O–H bond cleavage in the key step of FA deprotonation in $Au–ZrO_2$ interface resulting in high catalytic activity. The dimethylethanolamine showed the most promoting effect on FA-amine adducts dehydrogenation under ambient conditions due to its unique tertiary structure which could easy interact with FA molecules in deprotonation process. The $Au/ZrO_2$ catalyst also exhibited excellent stability for dimethylethanolamine-assisted FA dehydrogenation whether or in large-scale system. Considering the exceptional activity of amine with high boiling point promoted hydrogen generation from FA-amine adducts using $Au/ZrO_2$ catalyst, the present findings can provide a new way to design and develop highly efficient process for sustainable and clean energy production and chemical synthesis.

## Acknowledgment

This research was financially supported by the National Natural Science Foundation of China (21273044, 21473035, 91545108 and 51502331) and the Science and Technology Commission of Shanghai (Grant 16ZR1440400).

## REFERENCES

[1] Enthaler S. Carbon dioxide—the hydrogen-storage material of the future? ChemSusChem 2008;1:801–4.
[2] Joó F. Breakthroughs in hydrogen storage—formic acid as a sustainable storage material for hydrogen. ChemSusChem 2008;1:805–8.
[3] Yu KMK, Curcic I, Gabriel J, Tsang SCE. Recent advances in $CO_2$ capture and utilization. ChemSusChem 2008;1:893–9.
[4] Jiang HL, Singh SK, Yan JM, Zhang XB, Xu Q. Liquid-phase chemical hydrogen storage: catalytic hydrogen generation under ambient conditions. ChemSusChem 2010;3:541–9.
[5] Schlapbach L, Züttel A. Hydrogen-storage materials for mobile applications. Nature 2001;414:353–8.
[6] Aresta M, Dibenedetto A, Angelini A. Catalysis for the valorization of exhaust carbon: from $CO_2$ to chemicals,

materials, and fuels. Technological use of CO2. Chem Rev 2014;114:1709–42.
[7] Moriarty P, Honnery D. Hydrogen's role in an uncertain energy future. Int J Hydrogen Energy 2009;34:31–9.
[8] Eberle U, Felderhoff M, Schüth F. Chemical and physical solutions for hydrogen storage. Angew Chem Int Ed 2009;48:6608–30.
[9] van den Berg AWC, Areán CO. Materials for hydrogen storage: current research trends and perspectives. Chem Commun 2008;6:668–81.
[10] Weidenthaler C, Felderhoff M. Solid-state hydrogen storage for mobile applications: Quo Vadis? Energy Environ Sci 2011;4:2495–502.
[11] Solymosi F, Koós Á, Liliom N, Ugrai I. Production of CO-free $H_2$ from formic acid. A comparative study of the catalytic behavior of Pt metals on a carbon support. J Catal 2011;279:213–9.
[12] Himeda Y. Highly efficient hydrogen evolution by decomposition of formic acid using an iridium catalyst with 4,4'-dihydroxy-2,2'-bipyridine. Green Chem 2009;11:2018–22.
[13] Tedsree K, Kong ATS, Tsang SC. Formate as a surface probe for ruthenium nanoparticles in solution $^{13}C$ NMR spectroscopy. Angew Chem Int Ed 2009;48:1443–6.
[14] Ojeda M, Iglesia E. Formic acid dehydrogenation on Au-based catalysts at near-ambient temperatures. Angew Chem Int Ed 2009;48:4800–3.
[15] Tedsree K, Chan CWA, Jones S, Cuan Q, Li WK, Gong XQ, et al. $^{13}C$ NMR guides rational design of nanocatalysts via chemisorption evaluation in liquid phase. Science 2011;332:224–8.
[16] Karatas Y, Bulut A, Yurderi M, Ertas IE, Alal O, Gulcan M, et al. PdAu-$MnO_x$ nanoparticles supported on amine-functionalized $SiO_2$ for the room temperature dehydrogenation of formic acid in the absence of additives. Appl Catal B 2016;180:586–95.
[17] Hu C, Ting SW, Tsui J, Chan KY. Formic acid dehydrogenation over PtRuBi$O_x$/C catalyst for generation of CO-free hydrogen in a continuous-flow reactor. Int J Hydrogen Energy 2012;37:6372–80.
[18] Gazsi A, Schubert G, Pusztai P, Solymosi F. Photocatalytic decomposition of formic acid and methyl formate on $TiO_2$ doped with N and promoted with Au. Production of $H_2$. Int J Hydrogen Energy 2013;38:7756–66.
[19] Wang ZL, Ping Y, Yan JM, Wang HL, Jiang Q. Hydrogen generation from formic acid decomposition at room temperature using a NiAuPd alloy nanocatalyst. Int J Hydrogen Energy 2014;39:4850–6.
[20] Mandal K, Bhattacharjee D, Dasgupta S. Synthesis of nanoporous PdAg nanoalloy for hydrogen generation from formic acid at room temperature. Int J Hydrogen Energy 2015;40:4786–93.
[21] Loges B, Boddien A, Junge H, Beller M. Controlled generation of hydrogen from formic acid amine adducts at room temperature and application in $H_2/O_2$ fuel cells. Angew Chem Int Ed 2008;47:3962–5.
[22] Fellay C, Dyson PJ, Laurenczy G. A viable hydrogen-storage system based on selective formic acid decomposition with a ruthenium catalyst. Angew Chem Int Ed 2008;47:3966–8.
[23] Maenaka Y, Suenobu T, Fukuzumi S. Catalytic interconversion between hydrogen and formic acid at ambient temperature and pressure. Energy Environ Sci 2012;5:7360–7.
[24] Hull JF, Himeda Y, Wang WH, Hashiguchi B, Periana R, Szalda DJ, et al. Reversible hydrogen storage using $CO_2$ and a proton-switchable iridium catalyst in aqueous media under mild temperatures and pressures. Nat Chem 2012;4:383–8.
[25] Grasemann M, Laurenczy G. Formic acid as a hydrogen source—recent developments and future trends. Energy Environ Sci 2012;5:8171–81.
[26] Boddien A, Mellmann D, Gärtner F, Jackstell R, Junge H, Dyson PJ, et al. Efficient dehydrogenation of formic acid using an iron catalyst. Science 2011;333:1733–6.
[27] Bielinski EA, Lagaditis PO, Zhang Y, Mercado BQ, Würtele C, Bernskoetter WH, et al. Lewis acid-assisted formic acid dehydrogenation using a pincer-supported iron catalyst. J Am Chem Soc 2014;136:10234–7.
[28] Zhou X, Huang Y, Xing W, Liu C, Liao J, Lu T. High-quality hydrogen from the catalyzed decomposition of formic acid by Pd-Au/C and Pd-Ag/C. Chem Commun 2008;30:3540–2.
[29] Jones S, Qu J, Tedsree K, Gong XQ, Tsang SCE. Prominent electronic and geometric modifications of palladium nanoparticles by polymer stabilizers for hydrogen production under ambient conditions. Angew Chem Int Ed 2012;51:11275–8.
[30] Tedsree K, Li T, Jones S, Chan CWA, Yu KMK, Bagot PAJ, et al. Hydrogen production from formic acid decomposition at room temperature using a Ag-Pd core-shell nanocatalyst. Nat Nanotech 2011;6:302–7.
[31] Gu XJ, Lu ZH, Jiang HL, Akita T, Xu Q. Synergistic catalysis of metal–organic framework-immobilized Au-Pd nanoparticles in dehydrogenation of formic acid for chemical hydrogen storage. J Am Chem Soc 2011;133:11822–5.
[32] Chen Y, Zhu QL, Tsumori N, Xu Q. Immobilizing highly catalytically active noble metal nanoparticles on reduced graphene oxide: a non-noble metal sacrificial approach. J Am Chem Soc 2015;137:106–9.
[33] Zhu QL, Tsumori N, Xu Q. Immobilizing extremely catalytically active palladium nanoparticles to carbon nanospheres: a weakly-capping growth approach. J Am Chem Soc 2015;137:11743–8.
[34] Jiang K, Xu K, Zou S, Cai WB. B-doped Pd catalyst: boosting room-temperature hydrogen production from formic acid-formate solutions. J Am Chem Soc 2014;136:4861–4.
[35] Cai YY, Li XH, Zhang YN, Wei X, Wang KX, Chen JS. Highly efficient dehydrogenation of formic acid over a palladium-nanoparticle-based mott-schottky photocatalyst. Angew Chem Int Ed 2013;52:11822–5.
[36] Zhang S, Metin Ö, Su D, Sun S. Monodisperse AgPd alloy nanoparticles and their superior catalysis for the dehydrogenation of formic acid. Angew Chem Int Ed 2013;52:3681–4.
[37] Wang ZL, Yan JM, Ping Y, Wang HL, Zheng WT, Jiang Q. An efficient CoAuPd/C catalyst for hydrogen generation from formic acid at room temperature. Angew Chem Int Ed 2013;52:4406–9.
[38] Bi QY, Lin JD, Liu YM, Du XL, Wang JQ, He HY, et al. An aqueous rechargeable formate-based hydrogen battery driven by heterogeneous Pd catalysis. Angew Chem Int Ed 2014;53:13583–7.
[39] Liu Q, Yang X, Huang Y, Xu S, Su X, Pan X, et al. A schiff base modified gold catalyst for green and efficient $H_2$ production from formic acid. Energy Environ Sci 2015;8:3204–7.
[40] Wang X, Qi GW, Tan CH, Li YP, Guo J, Pang XJ, et al. Pd/C nanocatalyst with high turnover frequency for hydrogen generation from the formic acid-formate mixtures. Int J Hydrogen Energy 2014;39:837–43.
[41] Liu J, Lan L, Li R, Liu X, Wu C. Agglomerated Ag-Pd catalyst with performance for hydrogen generation from formic acid at room temperature. Int J Hydrogen Energy 2016;41:951–8.
[42] Jeon M, Han DJ, Lee KS, Choi SH, Han J, Nam SW, et al. Electronically modified Pd catalysts supported on N-doped

carbon for the dehydrogenation of formic acid. Int J Hydrogen Energy 2016;41:15453–61.
[43] Yang L, Luo W, Cheng G. Monodisperse CoAgPd nanoparticles assembled on graphene for efficient hydrogen generation from formic acid at room temperature. Int J Hydrogen Energy 2016;41:439–46.
[44] Mao H, Huang T, Yu A. Electrochemical surface modification on CuPdAu/C with extraordinary behavior toward formic acid/formate oxidation. Int J Hydrogen Energy 2016;41:13190–6.
[45] Bi QY, Lin JD, Liu YM, He HY, Huang FQ, Cao Y. Gold supported on zirconia polymorphs for hydrogen generation from formic acid in base-free aqueous medium. J Power Sources 2016;328:463–71.
[46] Bi QY, Lin JD, Liu YM, He HY, Huang FQ, Cao Y. Dehydrogenation of formic acid at room temperature: boosting palladium nanoparticle efficiency by coupling with pyridinic-nitrogen-doped carbon. Angew Chem Int Ed 2016;55:11849–53.
[47] Li SJ, Ping Y, Yan JM, Wang HL, Wu M, Jiang Q. Facile synthesis of AgAuPd/graphene with high performance for hydrogen generation from formic acid. J Mater Chem A 2015;3:14535–8.
[48] Jiang Y, Fan X, Xiao X, Qin T, Zhang L, Jiang F, et al. Novel AgPd hollow spheres anchored on graphene as an efficient catalyst for dehydrogenation of formic acid at room temperature. J Mater Chem A 2016;4:657–66.
[49] Wang N, Sun Q, Bai R, Li X, Guo G, Yu J. In situ confinement of ultrasmall Pd clusters within nanosized silicalite-1 zeolite for highly efficient catalysis of hydrogen generation. J Am Chem Soc 2016;138:7484–7.
[50] Bi QY, Du XL, Liu YM, Cao Y, He HY, Fan KN. Efficient subnanometric gold-catalyzed hydrogen generation via formic acid decomposition under ambient conditions. J Am Chem Soc 2012;134:8926–33.
[51] Menegazzo F, Manzoli M, Chiorino A, Boccuzzi F, Tabakova T, Signoretto M, et al. Quantitative determination of gold active sites by chemisorption and by infrared measurements of adsorbed CO. J Catal 2006;237:431–4.
[52] Fang W, Chen J, Zhang Q, Deng W, Wang Y. Hydrotalcite-supported gold catalyst for the oxidant-free dehydrogenation of benzyl alcohol: studies on support and gold size effects. Chem Eur J 2011;17:1247–56.
[53] Liu SS, Liu X, Yu L, Liu YM, He HY, Cao Y. Gold supported on titania for specific monohydrogenation of dinitroaromatics in the liquid phase. Green Chem 2014;16:4162–9.
[54] Zhang H, Watanabe T, Okumura M, Haruta M, Toshima N. Catalytically highly active top gold atom on palladium nanocluster. Nat Mater 2012;11:49–52.
[55] Rogers SM, Catlow CRA, Chan-Thaw CE, Gianolio D, Gibson EK, Gould AL, et al. Tailoring gold nanoparticle characteristics and the impact on aqueous-phase oxidation of glycerol. ACS Catal 2015;5:4377–84.